*Received: 05 December 2018 Accepted: 07 February 2019* *DOI ID: 10.5505/jems.2019.30922*

Journal of ETA Maritime Science JEMS JOURNAL

Corresponding Author: Kubilay BAYRAMOĞLU

# Numerical and Theoretical Thermal Analysis of Ship Provision Refrigeration System

Kubilay BAYRAMOĞLU, Semih YILMAZ, Kerim Deniz KAYA

Dokuz Eylül University, Maritime Faculty, Turkey
*kubilay.bayramoglu@deu.edu.tr;* ORCID ID: https://orcid.org/0000-0002-5838-6132
*semih.yilmaz@deu.edu.tr;* ORCID ID: https://orcid.org/0000-0002-0791-4476
*deniz.kaya@deu.edu.tr;* ORCID ID: https://orcid.org/0000-0002-0985-2280

## *Abstract*

*The freezer system on ships involves provisions where meat, fish, vegetables etc. are cooled down. Provision room is one of the essential features on ships for the preservation of food. The size of the cooling chamber varies according to the length of the ship and the number of personnel. Under the scope of the study, a room with volume of 15 $m^3$ (H x L x W, 2.5 x 3 x 2 m.) has been designed for the preservation of the meat. Boundary conditions which are determined for numerical and theoretical analysis in provision room have been chosen considering existing ship conditions. Refrigeration load, temperature distribution and flow streamline to keep the meat at the desired temperature in the provision room have been analyzed for one hour working period. Within this time interval, average meat domain and air temperature drop have been found as 4.33 K and 13 K, respectively. CFD analysis and theoretical calculation results have been compared. The results have found to be in agreement with acceptable errors less than 10%. The outputs from analysis show that refrigeration unit provides suitable temperature decrease within determined time interval.*

***Keywords:*** *Refrigeration Systems, Computational Fluid Dynamics, Ship Provision Room.*

## Gemi Kumanya Odasının Sayısal ve Teorik Termal Analizi

## *Öz*

*Gemilerde et, balık ve meyve sebze gibi kumanyaların bulunduğu bölmelerin soğutularak muhafaza edildiği soğutma sistemleri mevcuttur. Gemilerde bulunan soğutma sistemi yiyeceklerin bozulmadan muhafaza edildiği temel ve gerekli yapılardan biridir. Bu soğutma odaları geminin boyuna ve bulunan mürettebat sayısına göre farklı boyutlara sahip olabilir. Çalışmada, 15 $m^3$ (Y x U x G, 2.5 x 3 x 2 m.) boyutlarında karkas etlerin korunması amacıyla bir oda tasarlanmıştır. Teorik ve sayısal çalışma için sınır koşulları uygun gemi koşulları düşünülerek belirlenmiştir. Soğutma odasında yer alan etin sıcaklığını istenilen değerde tutmak için soğutma yükü, sıcaklık dağılımı ve akış hattı bir saat süreyle zamana bağlı olarak analiz edilmiştir. Bu zaman aralığı için et kontrol hacmi ve soğutma odası havasındaki sıcaklık düşüş değeri sırasıyla 4.33 K ve 13 K olarak bulunmuştur. Çalışmada, sayısal analiz ve teorik hesaplama sonuçları karşılaştırılmıştır. Sonuçlar, %10 değerinden daha az bir hata payı ile doğrulanmıştır. Analiz çıktıları, soğutma odası için soğutma ünitesinin belirlenen zaman aralığında uygun sıcaklık düşümünü sağladığını göstermiştir.*

***Anahtar Kelimeler:*** *Soğutma Sistemi, Hesaplamalı Akışkanlar Dinamiği, Gemi Kumanya Odası.*

**To cite this article:** Bayramoğlu, K., Yılmaz, S. & Kaya, K. D. (2019). Numerical and Theoretical Thermal Analysis of Ship Provision Refrigeration System. *Journal of ETA Maritime Science*, 7(2), 137-149.
**To link to this article:** https://dx.doi.org/10.5505/jems.2019.30922

## 1. Introduction

Cooling rooms where food is kept without degeneration on ships are generally designed as three separate rooms. The first one of these rooms is called dry provision where dry foods such as potatoes are preserved. Dry provisions should not be cooled too much. Only, these rooms must be dehumidified. The other two rooms in the provision are the rooms where food such as meat and fish are stored [1].

The lack of effective food cooling systems causes changes in the structure of food [2]. Many ship provision products require refrigeration. Food should be stored at low temperatures to ensure that food on ships is protected from microscopic organisms that can cause adverse effects, such as bacteria. Frozen foods such as meat must be frozen in order to protect their initial properties while being carried inside the freezer for a long-term [3]. The meat storage temperature of the room should be lower than -12 ˚C degrees. Reaching such lower temperatures in these rooms creates various problems inside the ship environment [1, 4].

Refrigeration room is commonly designed for keeping foods at a certain temperature to convenient freshness, quality, safety, and shelf life. For this reason, the refrigeration system generally requires excellent optimization in ships. There are several factors that affect the cooling units such as indoor and outdoor operating conditions. Provision room has three main components; room cavity, insulated walls and refrigeration units. Airflow and heat transfer calculation inside the provision room is a very challenging task [5].

There are many approaches to solving refrigeration problems. Nowadays, experimental tests and computational analyses are mostly preferred by researchers. Experimental tests require plenty of time, expensive equipment and usually applied to simple problems [5-10]. The promising approach from computational analyses is computational fluid dynamics (CFD). The CFD model is the paramount option for the prediction and analysis of refrigeration systems [11]. CFD employs finite volume and finite element method. These methods convert all governing equations into algebraic form and allow them to be numerically solved [12].

Zhijuan et al. [13] investigated the relationship between food package temperature and internal environment. This study revealed that the temperature of the cooling cabinet is affected by light, outdoor airflow, and partial humidity. Ge et al. [11] applied 2D steady-state CFD model to investigate the airflow dynamics and heat transfer for airflow from cooling coil air off-to air-on and also numerical simulation results were tested with experimental results. Tsang and Yung [14] evaluated the factors that emerge freezing capacity loss. The researchers compared the regression model taken by experimental data with the theoretical formulation efficiency. Aste et al. [15] presented a comprehensive review of scientific and grey literature on active refrigeration technologies for food preservation. Glavan et al. [16] studied hybrid model of a refrigeration system. This system includes many different refrigeration models such as refrigerated display case dynamics, food dynamics, evaporation model and ice formation model. 3-D simulation model of full refrigeration cabinet was designed by Wang et al. [5]. CFD simulation of refrigeration model showed temperature distribution in refrigeration cabinet. Jolly et al. [17] studied a shipping container refrigeration system with a mathematical model and investigated thermal performance for full load simulation. Getahun et al. [18] developed and validated a CFD model for a refrigerated shipping container with a porous medium approach. An open

refrigerated display cabinet (ORDC) was investigated by Carvalho et al. [19] with airflow and heat transfer CFD modelling.

In the present study, fluid flow and heat transfer modelling of refrigerated provision room is performed by CFD with commercial software ANSYS Fluent® [20]. The theoretical model is created by heat transfer and refrigeration load calculation equations. Comprehensive numerical model findings are compared with theoretical results. Besides that, temperature profiles in room air and meat are obtained in 3D space. Hence, the effect of location on the temperature profile in meat is clearly seen. Temperature results will help not only for proper storage and management of meat but also for optimum location of refrigeration units in places with different wall temperatures.

## 2. Description of Provision Room

3D model of the provision room which is cooled down to -10 °C with refrigeration unit and 3 x 3 array hanged meat carcass are represented. Meat domain is designed by closest geometric shape shown in Figure 1. The inner structure of meat solid domain is assumed to be homogenous.

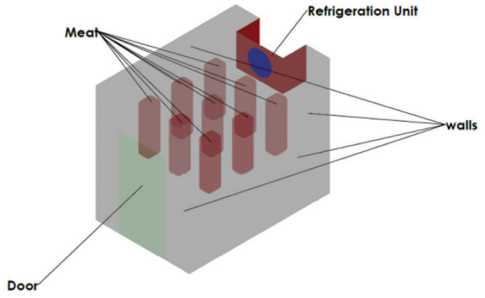


***Figure 1.*** *Provision Room 3D Detail*

Provision room geometry is designed with 2.5 m height, 3 m length and 2 m width considering the systems currently used on ships. Total weight of meat domains in simulation is determined to be 665 kg. The distance between the meat domains is 400 mm, placed in the middle of the room depending on the location of the evaporator. The position of the door to the provision room is defined as far away from the evaporator as possible in the computational domain.

The refrigeration unit is selected as single fan evaporator in the provision room the technical specifications of which are indicated in Table 1.

***Table 1.*** *Refrigeration Unit (Evaporator) Technical Specifications*

| Technical Specification | Values |
|---|---|
| Airflow rate [$m^3/h$] | 6000 |
| Fan diameter [mm] | 500 |
| Surface [$m^2$] | 26.1 |
| Average capacity [W] | 4600 |
| Defrost electrical heaters [W] | 10 x 500 |
| Dimensions (H x L x W) [mm] | 670 x 980 x 720 |

Generally, refrigerated room walls are insulated by sandwich panels in which polyurethane foam thicknesses can change according to heat insulation capacity, depending on the conditions of the region and the intended use of the structure. The sandwich panels are coated with metal sheets in compliance with TS EN ISO 6946 standards. The thickness of the enclosing plate is 0.5 mm and the thickness of the insulation walls (polyurethane) is 50 mm. The section of the walls is shown in Figure 2.

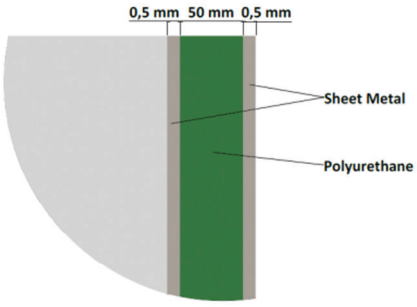


***Figure 2.*** *Provision Room Wall Section*

## 3. Theoretical Model

### 3.1. Heat Dissipation Over Walls

The heat exchange phenomenon takes place in many places of the cooling system when the cooling process is performed. In provision room walls, heat transfer calculation is made by thermal resistance network approach. Although the provision room is three-dimensional, approximate solutions can be achieved by assuming one-dimensional heat transfer [21]. In refrigeration systems, one-dimensional heat transfer is calculated by the following formula [22]:

$$Q=\frac{T_{\infty}-T_{\infty 2}}{\sum R_t} \quad (W) \tag{1}$$

$$\sum R_t=\frac{1}{h_1 A}+\frac{L_1}{k_1 A}+\frac{L_2}{k_2 A}+\frac{L_3}{k_3 A}+\frac{1}{h_2 A} \quad (K/W) \tag{2}$$

Provision room wall layers are made from two different materials. Heat transfer resistance network of walls is shown in Figure 3.

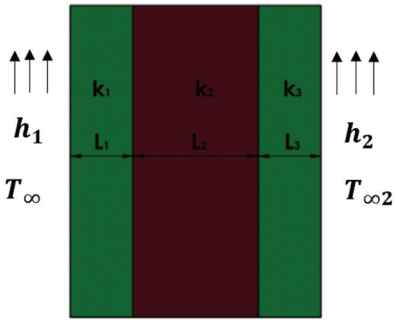


***Figure 3.*** *Equivalent Thermal Circuit for A Series of Composite Wall*

Total heat transfer coefficient (U) is defined for composite material walls with this formula:

$$U=\frac{1}{\sum R_t A} \quad (W/m^2 \cdot K) \tag{3}$$

### 3.2. Refrigeration Load Calculation

The purpose of the refrigeration load calculation is to select proper refrigeration system components in an economical manner. The correct choice of the refrigeration components will bring seamless and maintenance-free operation in provision refrigeration systems. The gains that resulted from heat form refrigeration loads. These loads can be categorized into four groups as follows [4]:

- Heat dissipation over walls, ceiling, and floor,
- Infiltration heat is caused by the external warm environment,
- Foods inside the cooled provision room,
- Heat sources like working humans, illumination, motors, etc.

It is desirable that the transmitted heat is very small in order to prevent the heat energy in the room from leaking out to the outside as described in the above section. In order to calculate the transmitted heat, the cooling room insulation thickness and type, the construction of the building, the physical properties of the volume to be cooled, the room volume and the volume effect outside must be determined in advance. Decreasing the coefficient of thermal conductivity and the cooling load can be achieved by increasing the insulation thickness but this thickness increases the cost and reduces the food storage volume [4].

Each time the cold room door is opened and closed, some external hot air enters the cold room creating an additional cooling load. It is possible to detect this load correctly, by knowing the actual operating conditions. Experimental studies have shown that the infiltration load depends on room volume in cooling applications. The influence of the infiltration load was neglected because the door of the ship provision room door was not used frequently (once a week) during operation.

Heat emerges from various species of foods that are stored in the ship provision room. This heat is the most important and largest part of the cooling load. Analytical heat transfer analysis can be applied with Fourier series for only very limited positions due to the complexity of the

three-dimensional transient heat transfer. In short, the determination of the cooling time depends on the type of the object to be cooled, the shape, the speed of the cold air given by the cooler, air temperature and distribution in the cold room and also the type of the cooling application.

The cooling load which is brought by the foods placed in the provision room is divided into four phases:

- Cooling over freezing temperature
- Latent heat to be taken during freezing
- Taking maturation heat of foods
- Super cooling after freezing

In this study, the provision room is kept at a certain temperature. The frozen meat is brought from outside to the provision room. Thus, super cooling after freezing is taken into consideration on analytical analysis as shown in the following equation:

$$Q_{fr} = \frac{m(kg)\cdot c_{meat}\ (kJ/kg\cdot K)\cdot \Delta T}{\text{Cooling Time(s)}}\ (kW) \qquad (4)$$

Lighting heat load is calculated according to lighting fixture type and operation time:

$$Q_{lf} = \frac{\text{Lighting Power (W) x Lighting Time(h)}}{\text{Operation Time (h)}}\ (kW) \qquad (5)$$

Another aspect in the refrigeration system during a long-time operation is defrosting. Defrost is caused by accumulated clogging of the outdoor heat exchanger (condenser). Airflow rate decrease of the evaporator fan trigger heat transfer performance drop in the cooling system [23, 24]. The electric defrost heaters in the cooled volume are located on the evaporator. Given the power of these heaters in Watt and the number of working hours per day, the heat which is emerged during the defrost can be found by the following equation [4]:

$$Q_{Def} = n \text{ x heat power x } H \text{ x } F\ (W) \qquad (6)$$

Where; n, number of defrost heater, H, running time of cooling (h/day) and F, defrost factor which is identified as a part of electrical energy entering the cooling room as heat load. Refrigeration load can be calculated with the following equation:

$$Q_t = Q + Q_{fr} + Q_{lf} + Q_{Def} \qquad (7)$$

## 4. Numerical Model

Numerical solutions of the physical process such as heat transfer, fluid flow, and other related process have been expressed in a mathematical form which is derived by governing differential equations. A computer program is often needed because it is difficult to solve these equations numerically [25]. A steady-state 3-D CFD model is solved using the commercial ANSYS Fluent® software package. This software is used to analyse the mathematical description of physical phenomena [26].

### 4.1. Governing Equations

In this study, incompressible flows are used for analysis and CFD solves conservation equations for mass and momentum. The conservation equations are relevant to turbulence modelling and heat transfer [20, 27]. The continuity equation can be written as follows;

$$\frac{\partial \rho}{\partial t} + \nabla\cdot(\rho\vec{v}) = 0 \qquad (8)$$

Where, ρ is the density and $\vec{v}$ is the velocity. In addition to above equation, gravity term is added in the body force. Conservation of momentum differential equation is given for a non-accelerating reference frame as follows [20, 25, 28].

$$\frac{\partial}{\partial t}(\rho\vec{v}) + \nabla\cdot(\rho\vec{v}\vec{v}) = -\nabla p + \nabla\cdot(\vec{\tau}) + \rho\vec{g} + \vec{F} \qquad (9)$$

$$\frac{\partial}{\partial t}(\rho H) + \nabla(\rho\vec{v}H) = \nabla\left(\frac{k}{c_p}\nabla H\right) \qquad (10)$$

where, p, $\vec{\tau}$, $\rho\vec{g}$, $\vec{F}$, H, T, k, and $c_p$ static pressure, stress tensor, gravitational body force, external body forces, enthalpy,

temperature, thermal conductivity and specific heat of air, respectively.

The standard k-ω turbulence model which is based on transport equations for the turbulence kinetic energy (k) and the specific dissipation rate (ω) has been used in the present study.

### 4.2. Mesh and Boundary Conditions

Three-dimensional fluid domain and computational mesh of the provision room is shown in Figure 4. In this model, boundaries of the refrigeration unit and meat have been intensified to take the most precise results. 5 boundary layers with 1.2 growth rate has been applied on meat surfaces. Meat domain and room domain has different element sizes on their bodies.

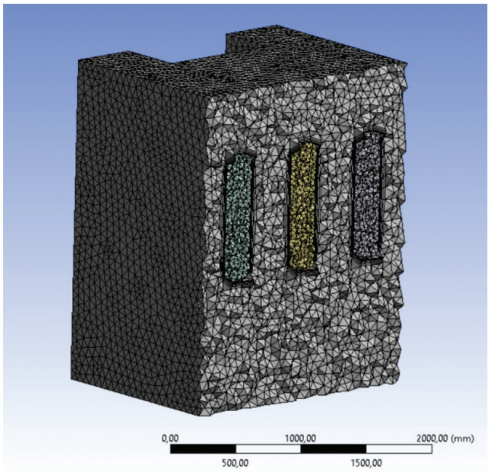


***Figure 4.*** *Computational Mesh*

Ansys Meshing commercial software has been used in mesh generation. Mesh dependence checks have been carried out for three different mesh models with various mesh densities. Temperature distribution on each meat domain has been calculated for 62243, 94356 and 456003 element numbers at 3600s. These numerical results show that the solution is independent of the mesh size both in solid and fluid regions as shown in Figure 5. According to effective use of computer resources and time, the grid that has 94356 elements is selected for the analysis. Mesh domain also contains structural and unstructured elements.

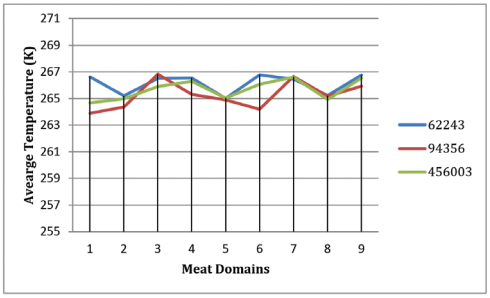


***Figure 5.*** *Grid Independency of Solid-Fluid Regions for 3600 s*

Second-order implicit time stepping method has been used with changeable step sizes of 0.02 and 0.2 up to 3600 s. A hundred iterations have been performed for each time step to achieve normalized residuals in the range of single precision machine accuracy. Mesh specifications are applied to the model are shown in Table 2.

***Table 2.*** *Mesh Specifications*

| Technical Specification | Values |
|---|---|
| Number of elements | 94356 |
| Element quality | 0.76226 |
| Mesh types | Tetrahedral and hexahedral mesh |

The creation of the appropriate numerical model in computational fluid dynamics applications is a very important factor. It is necessary to define the boundary conditions correctly on the created model in order to obtain correct results. In this study, the shape of three-dimensional CFD model for the provision room is shown in Figure 6.

To calculate the solutions, boundary conditions and material properties are applied in CFD software. Boundary conditions which have been determined considering provision room conditions are indicated in Table 3.

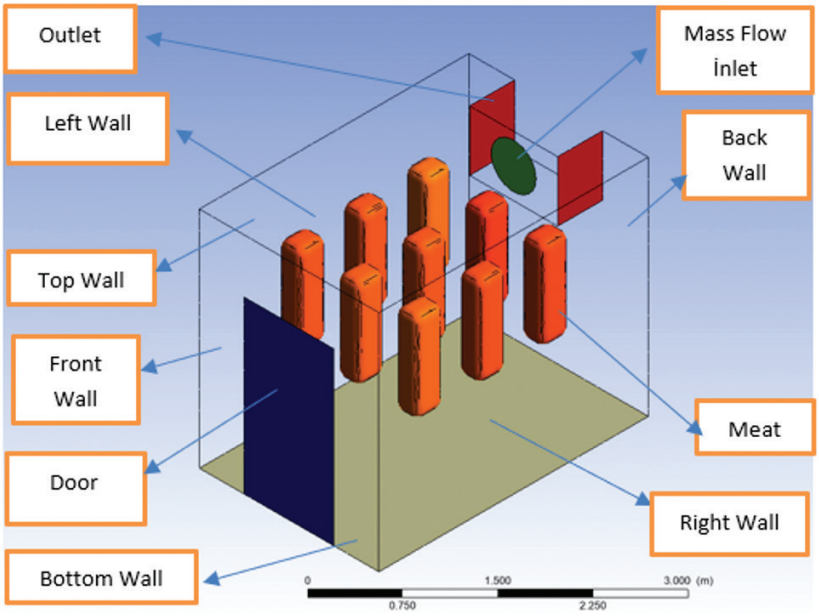


***Figure 6.*** *Boundary Conditions*

***Table 3.*** *Boundary Conditions*

| Types | Values |
|---|---|
| Mass flow inlet [kg/s] | 2.04 |
| Inlet temperature (°K) | 259 |
| Outlet | Pressure - Outlet |
| Wall heat transfer coefficient (W/m^2°K) | 0.412 |
| Wall (left, right, front, back and door) outside temperature (°K) | 313 |
| Wall (bottom and top) outside temperature (°K) | 303 |
| Provision room initial temperature (°K) | 273 |
| Meat initial temperature (°K) | 269 |

## 5. Results and Discussion

In ship provision refrigeration system, transport temperature of the food system must be at least -4 $^0$C (~269 K) to prevent food from spoiling. While setting initial conditions, provision room and blower (evaporator) inlet air temperature have been accepted to be 273 K and 259 K respectively. Data set values are taken by sample mid-planes. Locations of these planes are shown in the domain by Figure 7.

Temperature profile is a very important parameter for thermal uniformity in refrigeration analyses. In Figure 8, temperature distribution which is depending on determined operating conditions is calculated numerically for one hour working period. Plots are created with time intervals of 600 s, 1200 s, 1800 s, 2400 s, 3000 s and 3600 s, respectively.

Initially, the provision room and meat domain temperature are set to be 273 K and 269 K, respectively. According to temperature data at mid-plane 1, meat

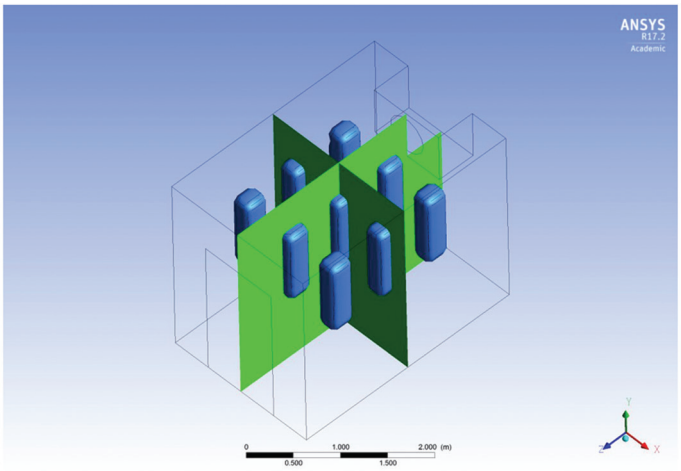


***Figure 7.*** *Dataset Plane Locations*

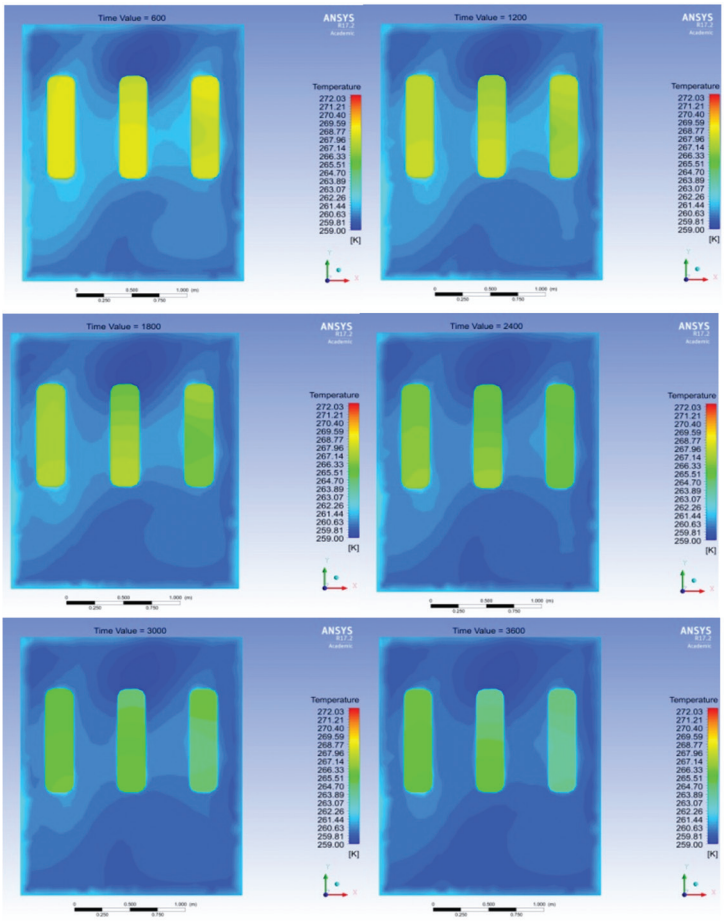


***Figure 8.*** *Temperature Distribution of Specified Time Intervals*

domain temperature decreases slowly over time after one-hour period. Meantime, average meat domain temperature drop is 4.33 K.

Similarly, meat domain temperature change is shown at mid-plane 2 in Figure 9. Temperature near the inlet is less than the provision room bottom side and also the temperature decreases because of the flow around the evaporator unit. Over one-hour period, average air temperature value has decreased by 13 K compared to the initial condition in the provision room, but the thermal uniformity could not be achieved.

Below the meat array since the cold air is blown over them. However, the velocity at the evaporator outlet is remarkably lower than the velocity at the evaporator inlet due to frictional loss of air through the circulation inside the room. After evaporator fan starts, air

begins to flow over meat domain and turns back to evaporator outlet. At t=1800 s, velocity profile of provision room is shown in Figure 10.

According to the analysis results, the highest velocity value occurs at the circumference of evaporator. Labelling for three dataset planes are shown with letters a, b, and c with the distance from refrigeration unit in Figure 11.

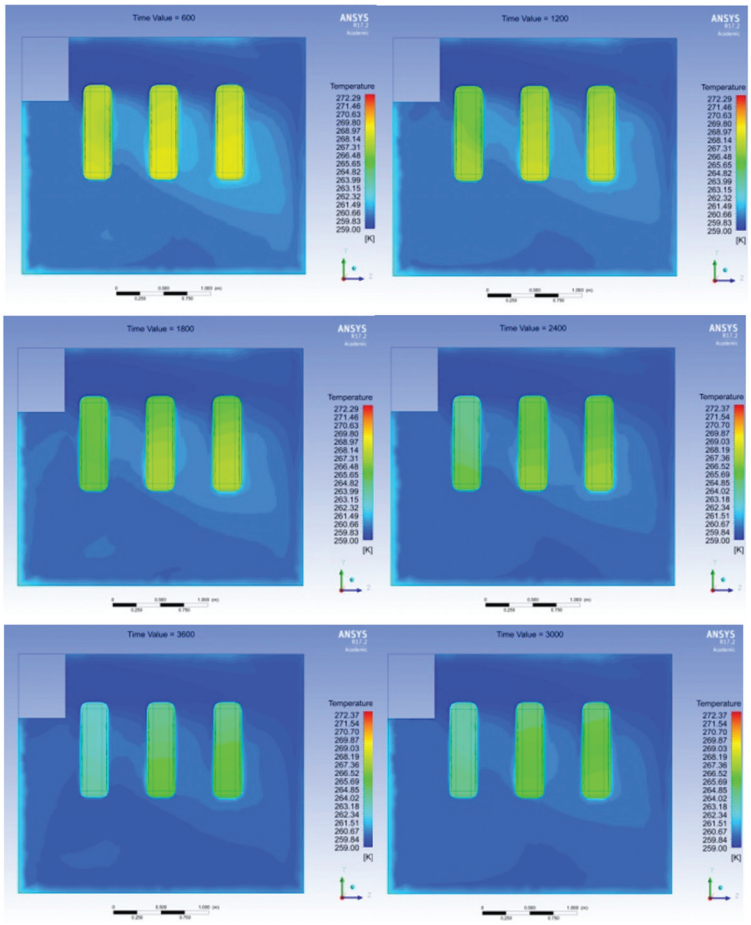


***Figure 9.*** *Temperature Distribution of Specified Time Intervals for mid-plane 2*

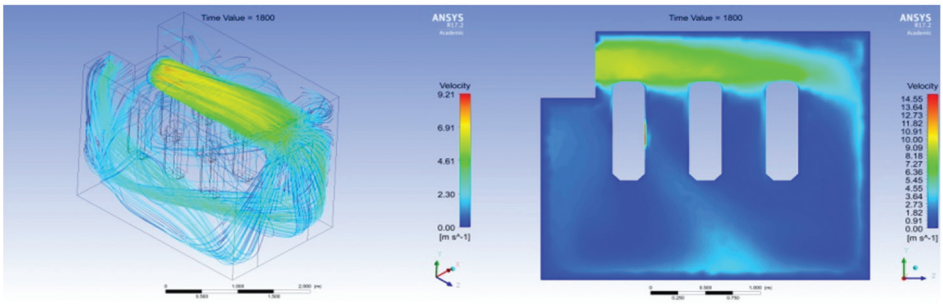


***Figure 10.*** *Velocity Profile of Provision Room (at t=1800 s)*

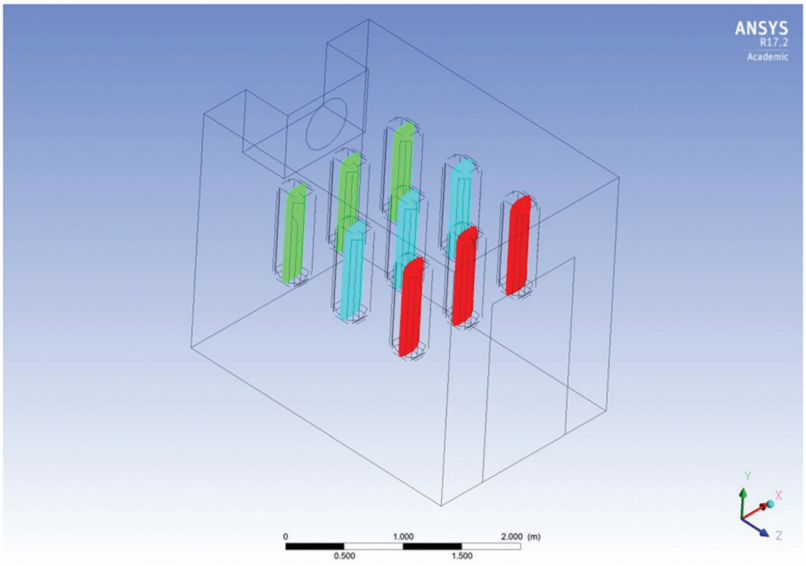


***Figure 11.*** *Labels for Dataset Plane Locations for Meat Domains*

Average temperature distributions in three dataset planes with their corresponding labels are shown in Figure 12. Temperatures shown are averaged in space at the time of 3600 s. It is observed that average temperature values for each plane are different from each other data received from the numerical analysis due to flow distribution in the provision room. The temperature values calculated for three different planes over one-hour working period are demonstrated in Figure 12.

Inside the provision room for a, b, c dataset planes at 3600 s., meat domain average temperatures decrease from 269 K to 264.76 K, 264.83 K and 264.50 K, respectively. According to these results, velocity streamlines of inlet fan, evaporator and meat positions have an influence on average temperatures of meat domains with respect to time.

Besides, CFD analysis and theoretical calculation results are compared and demonstrated in Table 4. According to heat transfer results, it can clearly be seen that analytical and numerical results are in good agreement with acceptable errors for each boundary condition. Theoretically calculated values of lighting and defrost are omitted in a numerical approach.

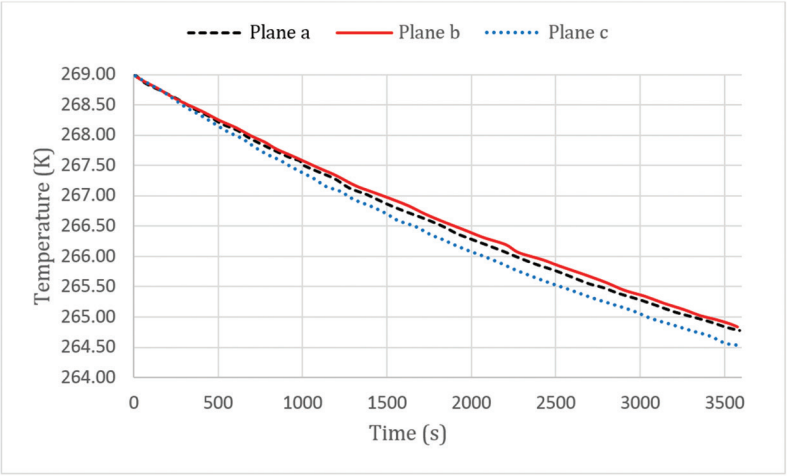


***Figure 12.*** *Meat Domain Temperature Profiles for a, b and c Planes*

***Table 4.*** *Heat Transfer on Boundary Conditions*

| Boundary Conditions | Analytical Results (W) | Numerical Results (W) | Error (%) |
|---|---|---|---|
| Meat (surface) | 1355.17 | 1242.1 | 8.34 |
| Wall (left and right) | 334.33 | 320.27 | 4.20 |
| Wall (back) | 96.73 | 91.34 | 5.57 |
| Wall (front) | 111.44 | 108.45 | 2.69 |
| Wall (top) | 99.89 | 96.14 | 3.75 |
| Wall (bottom) | 108.97 | 103.38 | 5.13 |

## 6. Conclusion

In this study, a three-dimensional ship provision system domain is analysed with analytical and numerical methods over transient operating conditions for one hour working period. 3D CFD Model has been generated with ANSYS® Fluent commercial software including airflow and heat transfer study in ship provision room.

Heat transfer on boundaries, temperature and velocity profiles on mid-planes are calculated over computational domain. According to the numerical results, average meat domain temperature and air temperature drop have been found to be 4.33 K and 13 K, respectively for one hour working period. However, it is observed that all meat domain average temperature changes are not the same inside the provision room.

The computed heat transfer for the present provision room geometry is compared with the analytical results. It can clearly be seen that CFD model heat transfer results, which are validated with theoretical findings, give less than 10% error.

This study shows that ship provision room temperature decreases over one hour working period depending on determined cooling capacity. Temperature decrease with respect to time is usable for choosing a suitable refrigeration system. Besides that, it leads to further improvements in the performance of ship provision room system designs. We suggest that further parametric studies are needed to investigate on refrigeration unit location inside the provision room.

## References


[1] Demirel, K. (2014). Gemi yardımcı makineleri ve Sistemleri. İstanbul: Birsen yayıncılık.

[2] Kayansayan, N., Alptekin, E., and Ezan, M.A. (2017). Thermal analysis of airflow inside a refrigerated container. International Journal of Refrigeration. 84 76–91.

[3] Pamuk, M.T., Savaş, A. (2017). A practical tool for evaluating refrigeration System using R-134a. Journal of ETA Maritime Science. 2017:5:1:69-79

[4] Özkol, N. (2016). Uygulamalı Soğutma Tekniği. Ankara: TMMOB Makine Mühendisleri Odası.

[5] Wang, L., Zhang, L., and Guoping, L. (2015). A CFD Simulation of 3D Airflow and Temperature Variation in Refrigeration Cabinet. Procedia Engineering, 2015:102:1599-1611.

[6] Marinetti, S., Cavazzini, G., Fedele, L., Zan, F., Schiesaro, P. (2012). Air velocity distribution analysis in the air duct of a display cabinet by PIV technique. International Journal of Refrigeration, 35:2312-2331.

[7] Yashar, D., Cho, H., Domanski, P. (2008). Measurement of air-velocity profiles for finned-tube heat exchangers using particle image velocimetry, in: International Refrigeration and Air Conditioning, Purdue University.

[8] Chen, Y., Yuan, X. (2005). Experimental study of the performance of single-band air curtains for a multi-deck refrigerated display cabinet, Journal of Food Engineering, 69 261-267.

[9] Field, B., Loth, E. (2006). Entrainment of refrigerated air curtains down a wall, Experimental Thermal and Fluid Science, 30:175-184.

[10] Yu, K., Ding, G., and Chen, T. (2009). Experimental investigation on a vertical display cabinet with central air supply, Energy Conversion and Management, 50:2257-2265.

[11] Ge, Y. T., Tassou, S. A. And Hadawey, A. (2010). Simulation of multi-deck medium temperature display cabinets with the integration of CFD and cooling coil models. Applied Energy. 87:10:3178-3188

[12] Ruangtrakoon, N., Thongtip, T., Aphornratana, S. and Sriveerakul, T. (2013). CFD simulation on the effect of primary nozzle geometries for a steam ejector in refrigeration cycle. international Journal of Thermal Sciences. 63:133-145

[13] Zhijuan, C., Xuehong, W., Yanli, L., Qiuyang, M. And Wenhui, Z. (2013). Numerical simulation on the food package temperature in refrigerated display cabinet influenced by indoor environment. Advances in Mechanical Engineering. 2013:7

[14] Tsang, A. H. F. and Yung, W. K. (2017). Development of an Adaptive Food Preservation System for food quality and energy efficiency enhancement. International Journal of Refrigeration, 76, 342–355.

[15] Aste, N., Del Pero, C., and Leonforte, F. (2016). Active refrigeration technologies for food preservation in humanitarian context - A review. Sustainable Energy Technologies and Assessments. 150-160

[16] Glavan, M., Gradišar, D., Invitto, S., Humar, I., Juričić, J., Pianese, C., and Vrančić, D. (2016). Cost optimisation of supermarket refrigeration system with hybrid model. Applied Thermal Engineering, 103, 56–66.

[17] Jolly, P. G., Tso, C. P., Wong, Y. W., & Ng, S. M. (2000). Simulation and measurement on the full-load performance of a refrigeration system in a shipping container. International Journal of Refrigeration, 23(2), 112–126.

[18] Getahun, S., Ambaw, A., Delele, M., Meyer, C. J. And Opara, U. L. (2017). Analysis of airflow and heat transfer inside fruit packed refrigerated shipping container: Part I Model development and validation. Journal of Food Engineering, 203, 58–68.

[19] Carvalho, C. C. de, Novaes, A. G., & Lima Júnior, O. F. (2010). a Logística Da Distribuição De Produtos Alimentícios Refrigerados: Problemas E Perspectivas No Contexto Brasileiro. XXVI Anpet, 1969–1980.

[20] Ansys Fluent User's Guide. (2016). ANSYS Inc., Release 17.2

[21] Çengel, Y.A. and Ghajar, A.J. (2015). Heat and Mass Transfer. New York: McGraw-Hill Education.

[22] Bergman, T.L., Lavıne, A.S., Incropera, F.P. and Dewitt, D.P. (2011). Fundamentals of Heat and Mass Transfer. USA: John Wiley & Son

[23] Kim, J., Choi, H. J., and Kim, K. C. (2015). A combined Dual Hot-Gas Bypass Defrosting method with accumulator heater for an air-to-air heat pump in cold region. Applied Energy. 147, 344–352.

[24] Song M, Xu X, Mao N, Deng S, Xu Y. 2017. Energy transfer procession in an air source heat pump unit during defrosting. Applied Energy. 204:679–689.

[25] Patankar, S.V. (1980). Numerical Heat transfer and Fluid Flow. USA: Hemisphere Publising Corparation.

[26] Parpas, D., Amaris, C., Sun, J., Tsamos, K. M., and Tassou, S. A. (2017). Numerical study of air temperature distribution and refrigeration systems coupling for chilled food processing facilities. Energy Procedia, 123, 156–163.

[27] Tanaka, F., Konishi, Y., Kuroki, Y., Hamanaka, D., and Uchino, T. (2012). The use of CFD to improve the performance of a partially loaded cold store. Journal of Food Process Engineering, 35(6), 874–880.

[28] Batchelor, G.K. (1967). An Introduction to Fluid Dynamics. England: Cambridge University Press.